leptoquark	decay	branching ratio	$\kappa 4\pi\alpha_{\rm em}$
S_{1L}	$e^+\bar{u}$	50%	$\frac{g_{1L}^2}{2}$
S_{1R}	$e^+\bar{u}$	100%	$\frac{g_{1R}^2}{2}$
$\tilde{S}_{1R}$	$e^+\bar{d}$	100%	$\frac{\tilde{g}_{1R}^2}{2}$
S_3^+	$e^+\bar{d}$	100%	g_3^2
S_3^0	$e^+\bar{u}$	50%	$\frac{g_3^2}{2}$
R_{2L}^1	$e^-\bar{u}$	100%	$\frac{h_{2L}^2}{2}$
R_{2R}^1	$e^-\bar{u}$	100%	$\frac{h_{2R}^2}{2}$
R_{2R}^2	$e^-\bar{d}$	100%	$\frac{h_{2R}^2}{2}$
$\tilde{R}_2^1$	$e^-\bar{d}$	100%	$\frac{\tilde{h}_{2L}^2}{2}$

TABLE I. Leptoquarks that can be observed through their decays into a $e^{\pm}$ and a jet and the correspondent branching ratios into this channel. We also show the relation between the leptoquark Yukawa coupling and the parameter κ used in PYTHIA.

Process	$\sigma_{\rm bare}$ (nb)	$\sigma_{\rm pair}$ (fb)
$q_i q_j \rightarrow q_i q_j$	1.0 10^2	4.8 10^2
$q_i \bar{q}_i \rightarrow q_k \bar{q}_k$	1.8	1.2 10^2
$q_i \bar{q}_i \rightarrow gg$	1.6	2.3
$q_i g \rightarrow q_i g$	6.2 10^2	1.0 10^3
$gg \rightarrow q_k \bar{q}_k$	25.	1.2 10^3
$gg \rightarrow gg$	6.9 10^2	5.5 10^2

TABLE II. Background processes included in the QCD class and their respective cross sections. To obtain σ_{bare} we required that the hard scattering process has $p_T > 100$ GeV; for σ_{pair} we further demanded that the $e^{\pm}$ have $p_T > 50$ GeV.

Process	$\sigma_{\rm bare}$ (pb)	$\sigma_{\rm pair}$ (fb)	ϵ_{12}	ϵ_{123}
$q_i\bar{q}_i \to g\gamma$	74.	0.14	0	0
$q_i\bar{q}_i \to gZ$	95.	$9.2\ 10^2$	1%	0.8%
$q_i\bar{q}_j \to gW^\pm$	$2.2\ 10^2$	8.8	0	0
$q_i\bar{q}_i \to \gamma Z$	1.4	16.	0.6%	0.4%
$q_i\bar{q}_j \to \gamma W^\pm$	1.1	$6.6\ 10^{-3}$	0	0
$q_i\bar{q}_i \to ZZ$	1.4	29.	0.8%	0.2%
$q_i\bar{q}_j \to ZW^\pm$	2.9	37.	1.2%	0.4%
$q_i\bar{q}_i \to W^+W^-$	6.8	38.	4.3%	4.3%
$q_ig \to q_i\gamma$	$6.1\ 10^2$	3.5	0	0
$q_ig \to q_iZ$	$5.5\ 10^2$	$5.4\ 10^3$	0.8%	0.2%
$q_ig \to q_kW^\pm$	$1.4\ 10^3$	$2.8\ 10^2$	0.25%	0.25%

TABLE III. Background processes included in the electroweak class and their respective cross sections with the same cuts used in Table II. We also exhibit the fraction of events ϵ_{12} (ϵ_{123}) that survive the cuts C1 and C2 (C1, C2, and C3); see text.

Process	$\sigma_{\rm bare}$ (pb)	$\sigma_{\rm pair}$ (fb)	ϵ_{12}	ϵ_{123}
$q_i q_j \to t q_k$	40.	11.	0.85%	0.01%
$q_i \bar{q}_i \to t\bar{t}$	0.40	$2.0\ 10^2$	0.40%	0.39%
$gg \to t\bar{t}$	$2.9\ 10^2$	$1.4\ 10^3$	75%	3.5%

TABLE IV. Background processes due to top quark production and their respective cross sections with the same cuts used in Table II. We also exhibit the fraction of events ϵ_{12} (ϵ_{123}) that survive the cuts C1 and C2 (C1, C2, and C3).

ℓq coupling	$M_{lq} = 500$ GeV	1000 GeV	1500 GeV	2000 GeV	2500 GeV
$e^{\pm} u$	$5.1\ 10^2$	27.	4.1	0.98	0.29
$e^{\pm} d$	$2.9\ 10^2$	14.	2.2	0.55	0.18

TABLE V. Total cross section in fb for the single production of a leptoquark that couples only to pair ℓq for several leptoquark masses. We required that the produced $e^{\pm}$ have $p_T > 50$ GeV, and that the scattering process has $p_T > 100$ GeV.

process	$M_{lq} = 500$ GeV	1000 GeV	1500 GeV	2000 GeV
$q\bar{q}$ fusion	86.	1.9	0.10	$2.7\ 10^{-3}$
gg fusion	$4.9\ 10^{2}$	6.3	0.25	$1.5\ 10^{-2}$

TABLE VI. Total cross section in fb for the pair production of leptoquarks, requiring that the produced $e^{\pm}$ have $p_T > 50$ GeV, and that the hard scattering process has $p_T > 100$ GeV.

M_{lq} (GeV)	ΔM (GeV)
300	50
500	50
1000	150
1500	200
2000	200
2500	300

TABLE VII. Invariant mass bins used in our analyses as a function of the leptoquark mass.

leptoquark	$\mathcal{L} = 10$ fb^{-1}	$\mathcal{L} = 100$ fb^{-1}
S_{1L} and S_3^0	1.1	1.5
S_{1R}, $\tilde{S}_{1R}$, R_{2L}^1,R_{2R}^2, and $\tilde{R}_2^1$	1.3	1.7

TABLE VIII. 95% CL limits on the leptoquark masses in TeV that can be obtained from the search for leptoquark pairs for two integrated luminosities.

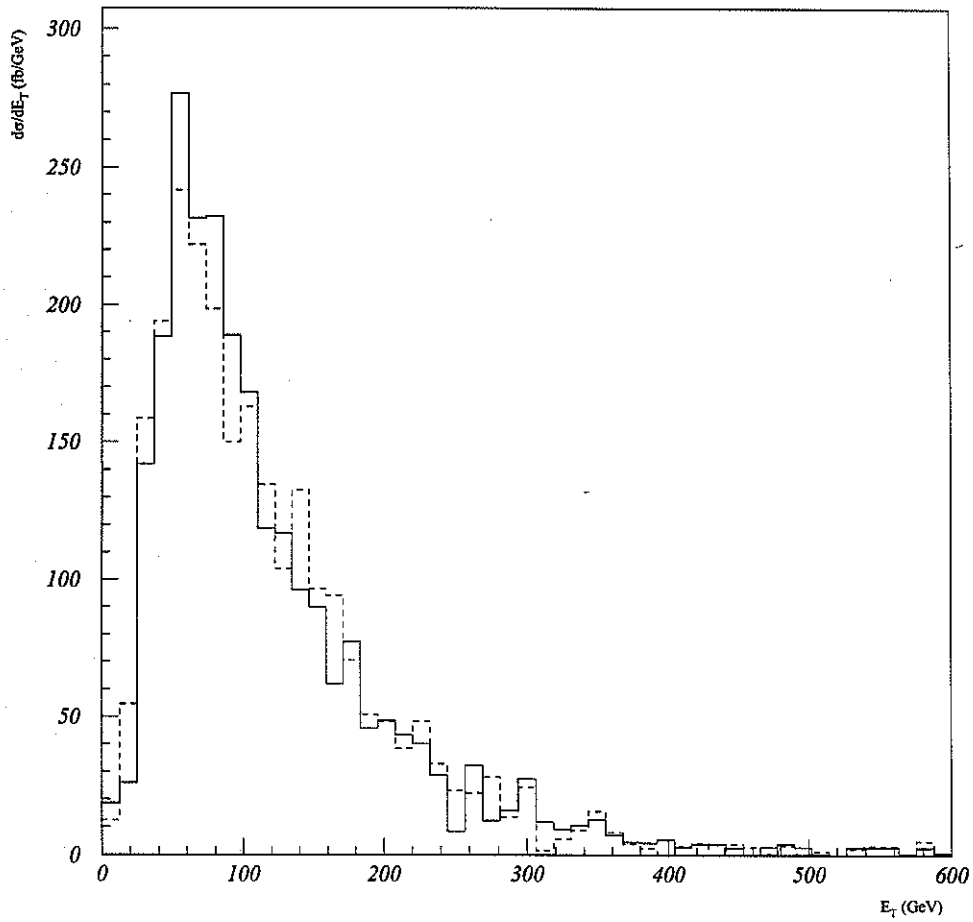

FIG. 1. Hadronic transverse energy deposited in a cone of size $\Delta R = 0.7$ around the direction of the e_1 (solid line) and the e_2 (dashed line) in QCD events.

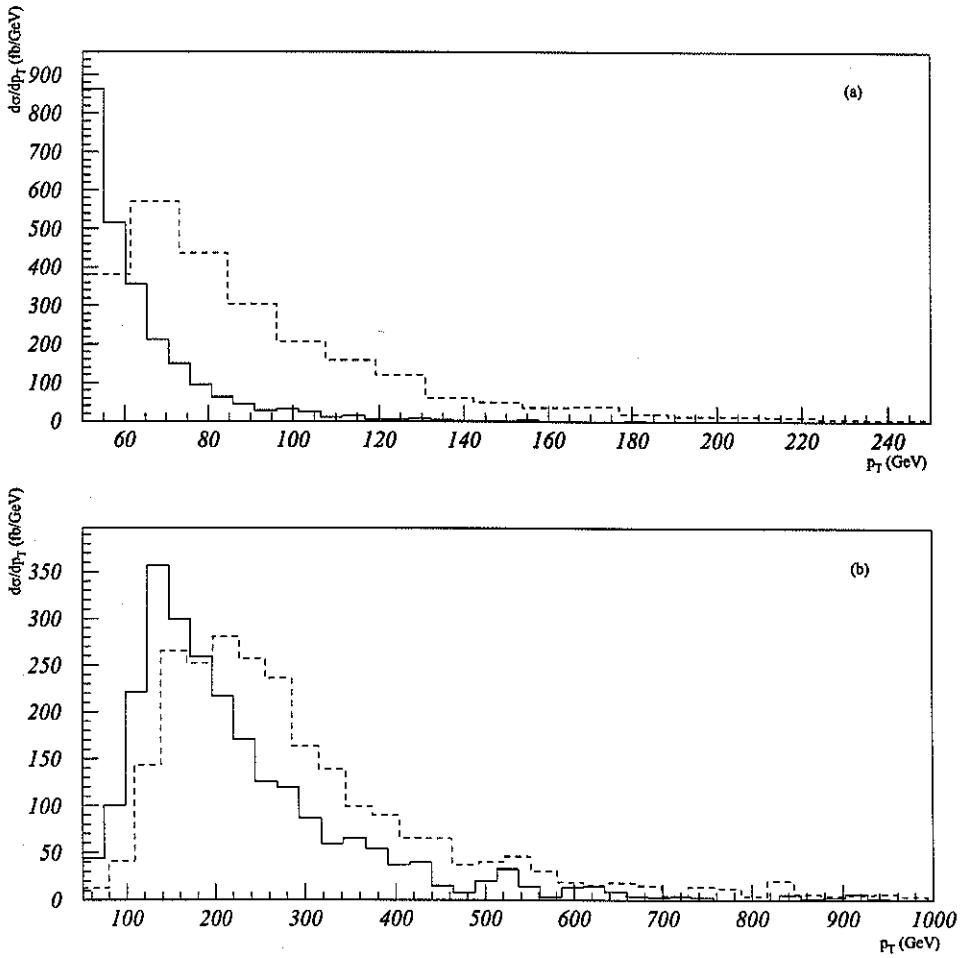

FIG. 2. For QCD events: (a) the dashed (solid) line stands for the p_T distribution of e_1 (e_2); (b) the dashed (solid) line stands for the p_T distribution of j_1 (j_2).

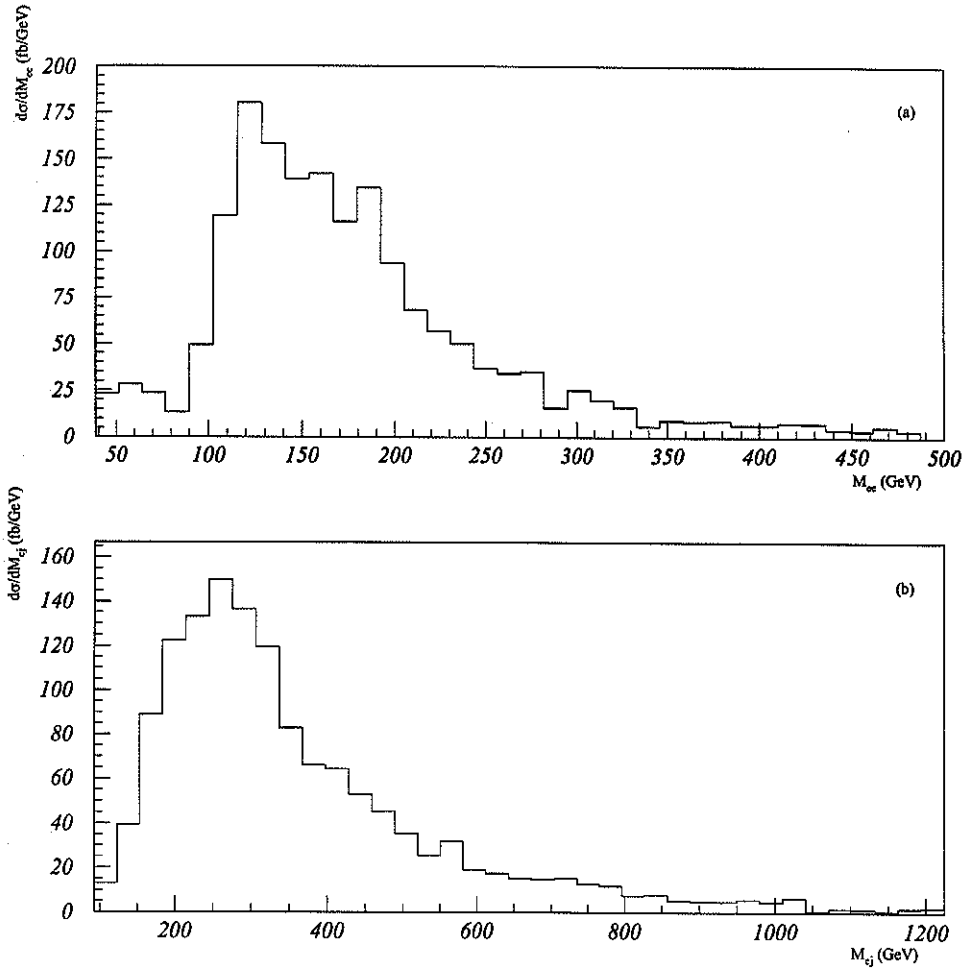

FIG. 3. For QCD events: (a) e_1e_2 invariant mass distribution; (b) $e^{\pm}$-jet invariant mass spectrum adding the 4 possible combinations.

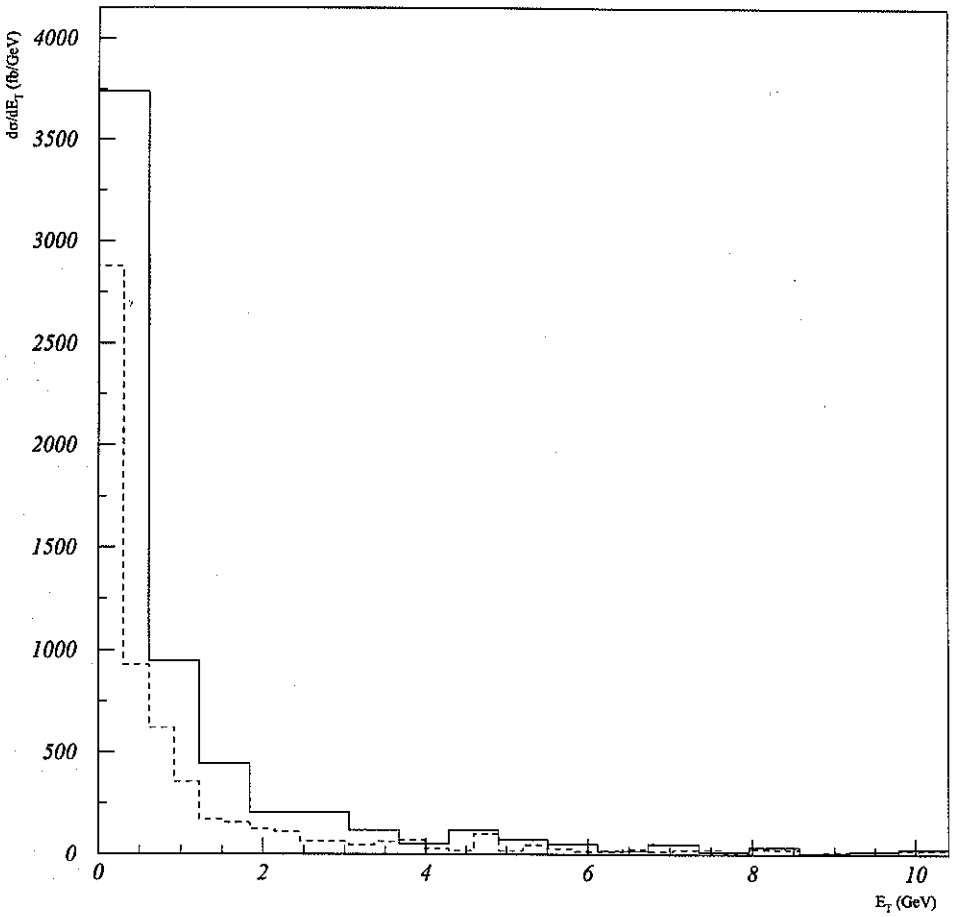

FIG. 4. The same distributions of Fig. 1 for electroweak events.

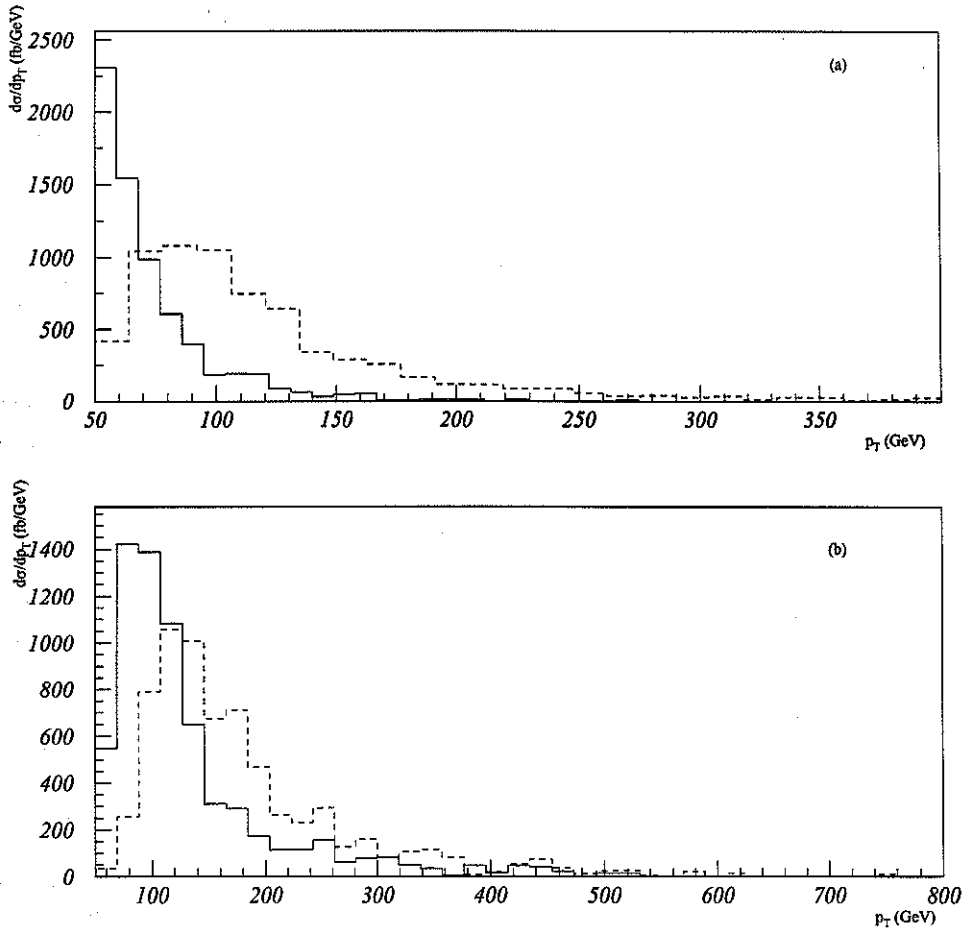

FIG. 5. The same distributions of Fig. 2 for electroweak events.

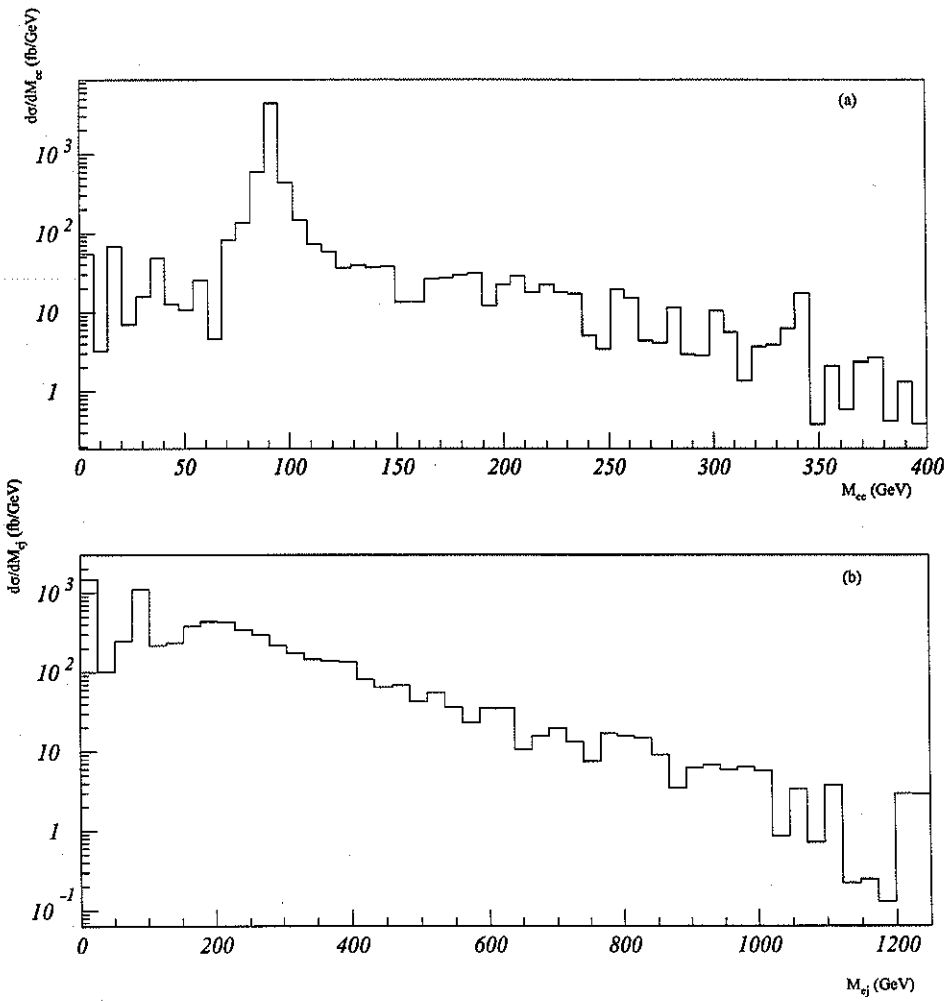

FIG. 6. The same distribution of Fig. 3 for electroweak events.

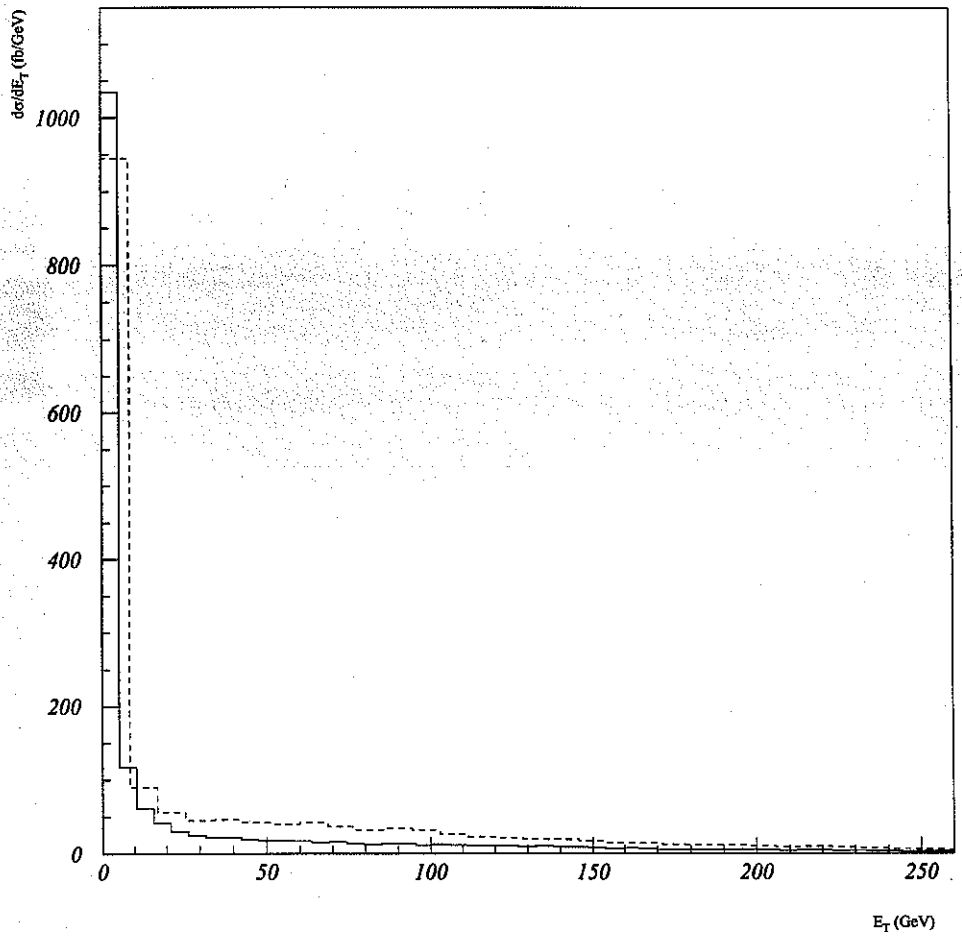

FIG. 7. The same distribution of Fig. 1 for top production.

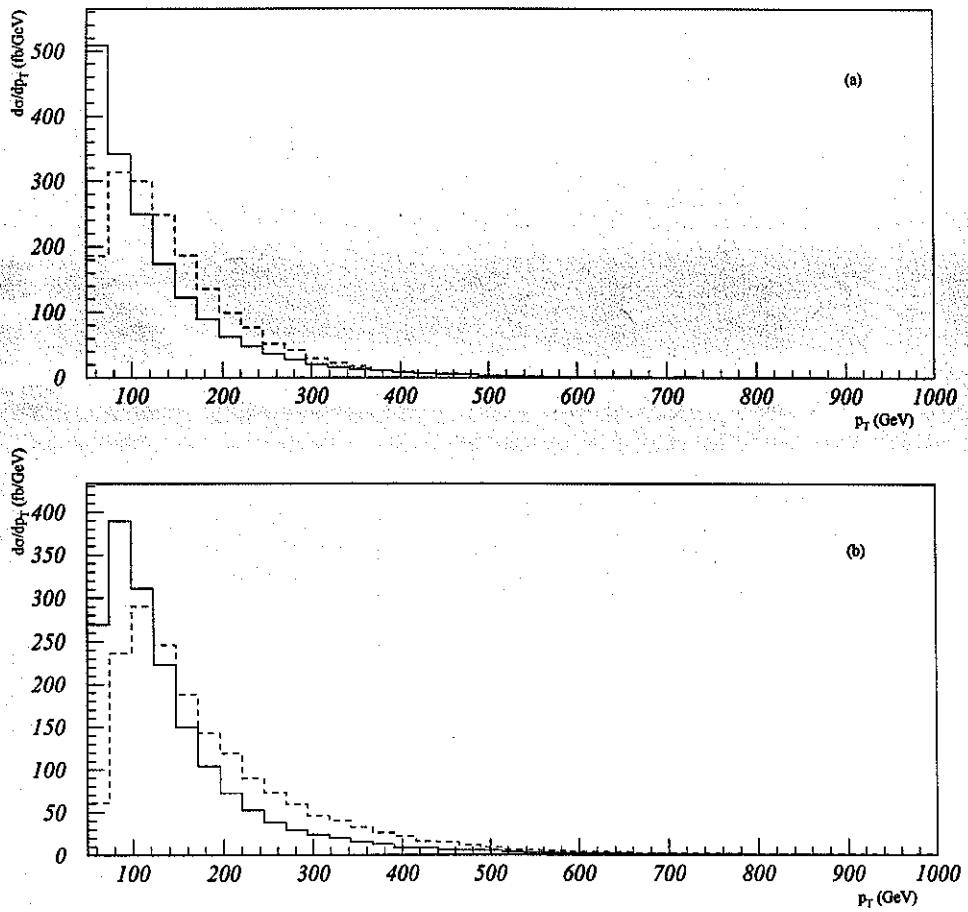

FIG. 8. The same distribution of Fig. 2 for top production.

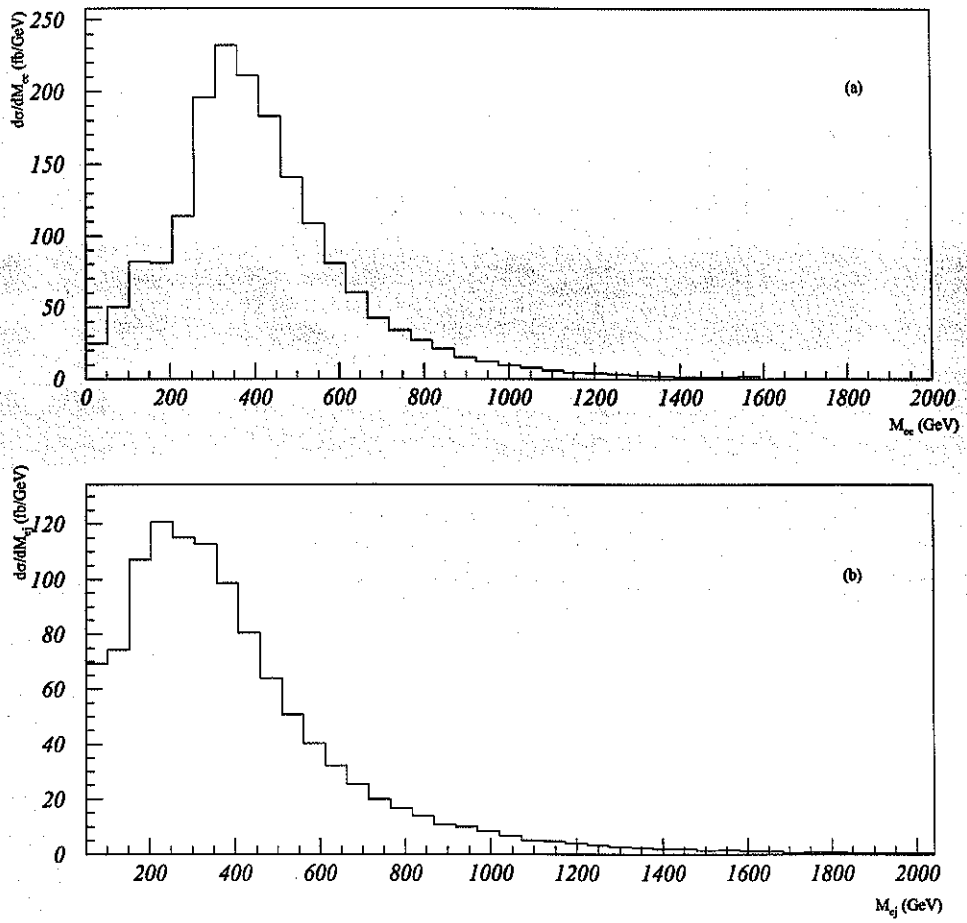

FIG. 9. The same distribution of Fig. 3 for top production.

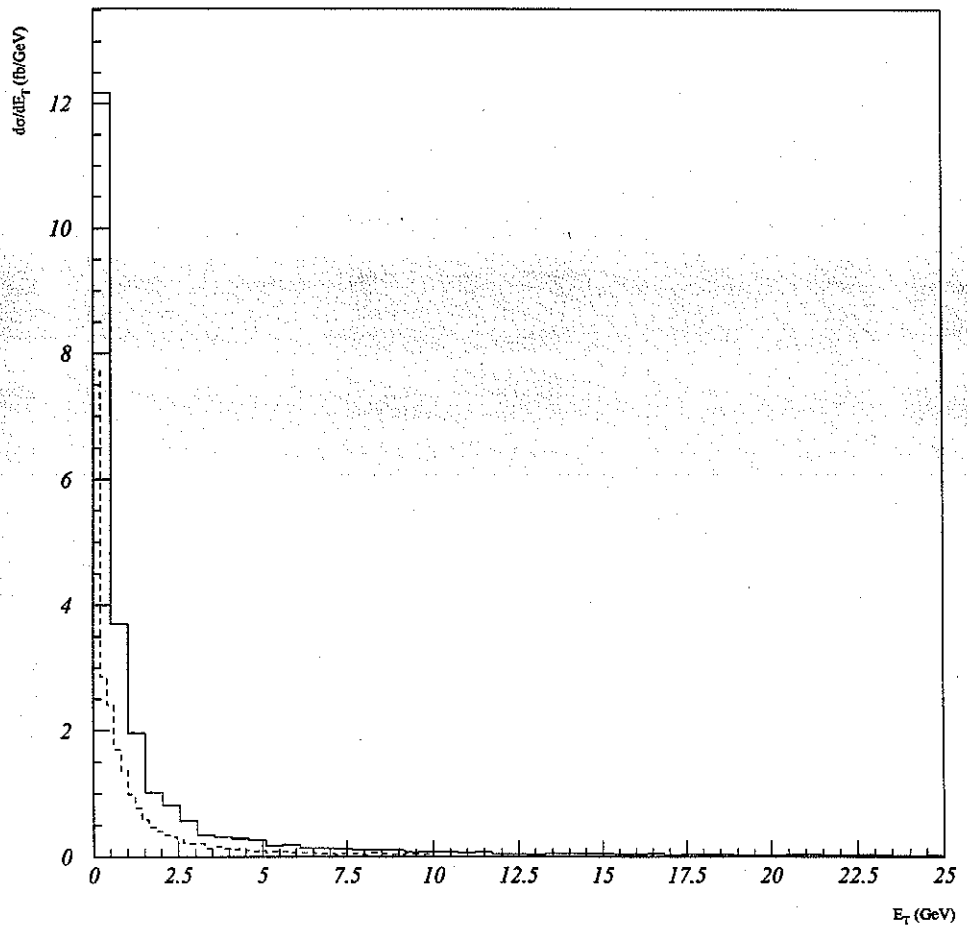

FIG. 10. The same distribution of Fig. 1 for the single production of $e^+\bar{u}$ leptoquarks of mass 1 TeV.

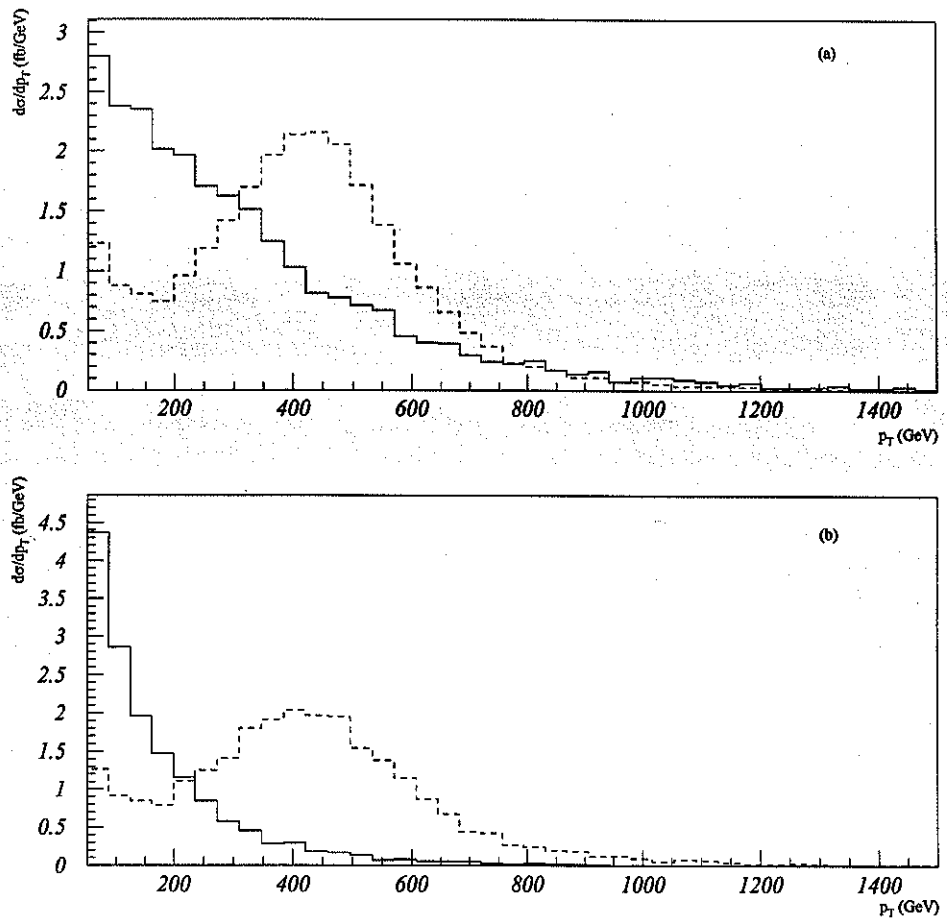

FIG. 11. The same distribution of Fig. 2 for the single production of $e^+\bar{u}$ leptoquarks of mass 1 TeV.

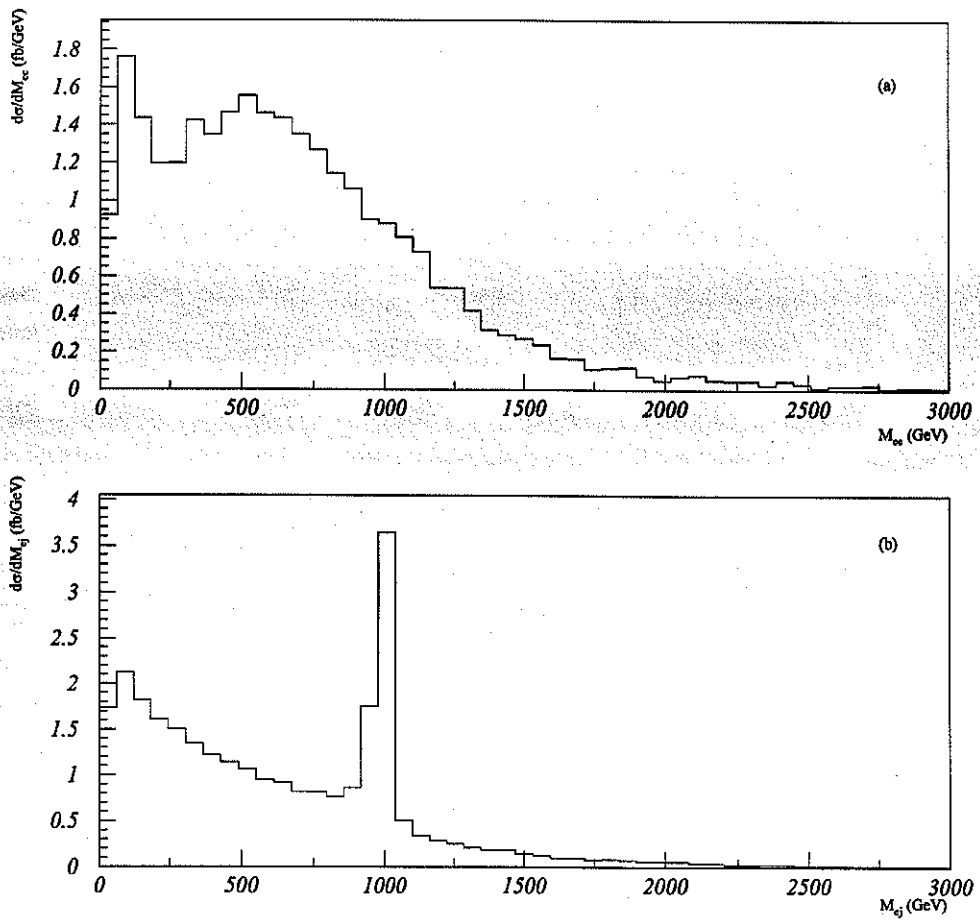

FIG. 12. The same distribution of Fig. 3 for the single production of $e^+\tilde{u}$ leptoquarks of mass 1 TeV.

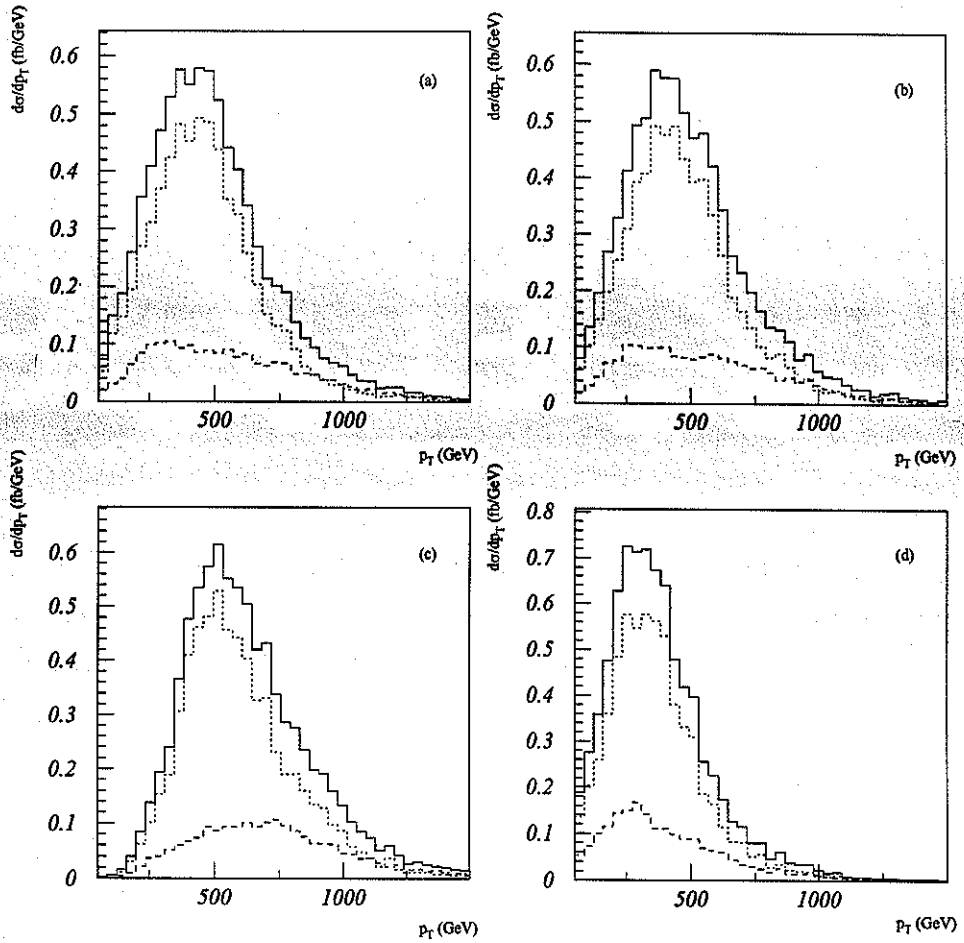

FIG. 13. p_T distribution of (a) e_1; (b) e_2; (c) j_1; (d) j_2; in the pair production of $e^+\bar{u}$ leptoquarks of mass 1 TeV. The dashed (dotted) line stands for the $q\bar{q}$- (gg-) fusion contribution while the solid line represents the total distribution.

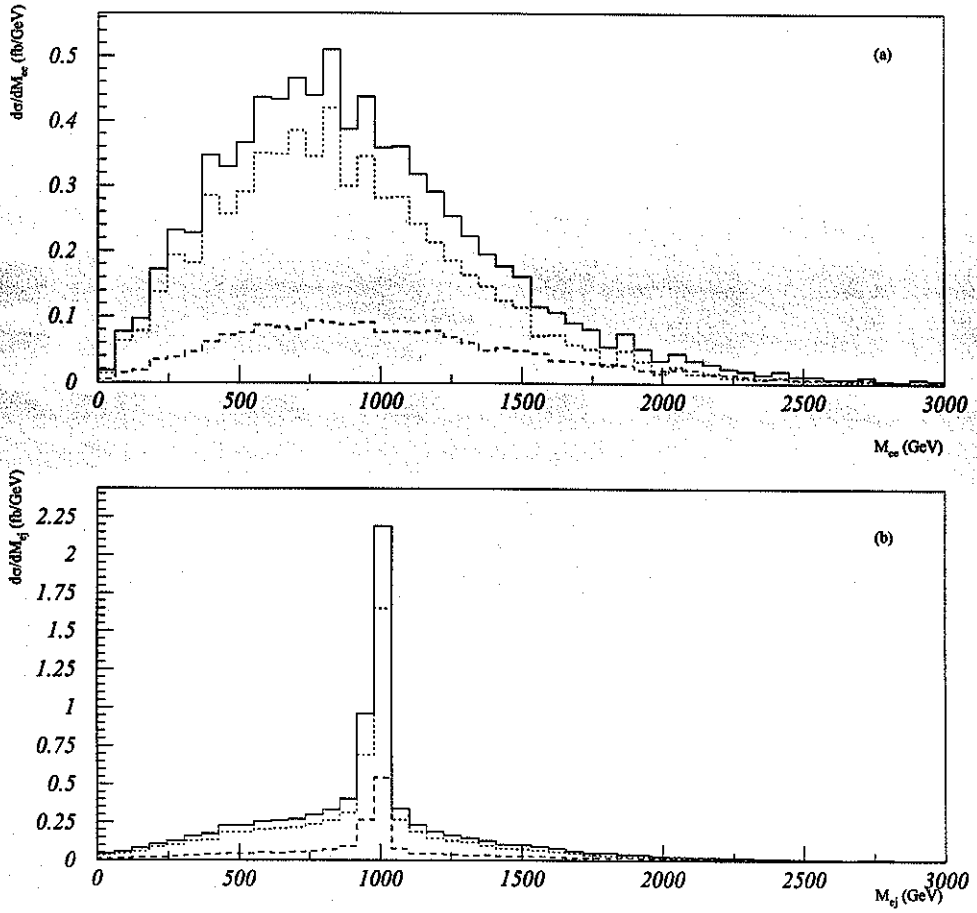

FIG. 14. (a) e^+e^- invariant mass distribution; (b) $e^{\pm}$-jet invariant mass spectrum adding the 4 possible combinations for pair production of $e^+\bar{u}$ leptoquarks with mass $M_{lq} = 1$ TeV. We use the conventions of Fig. 13.

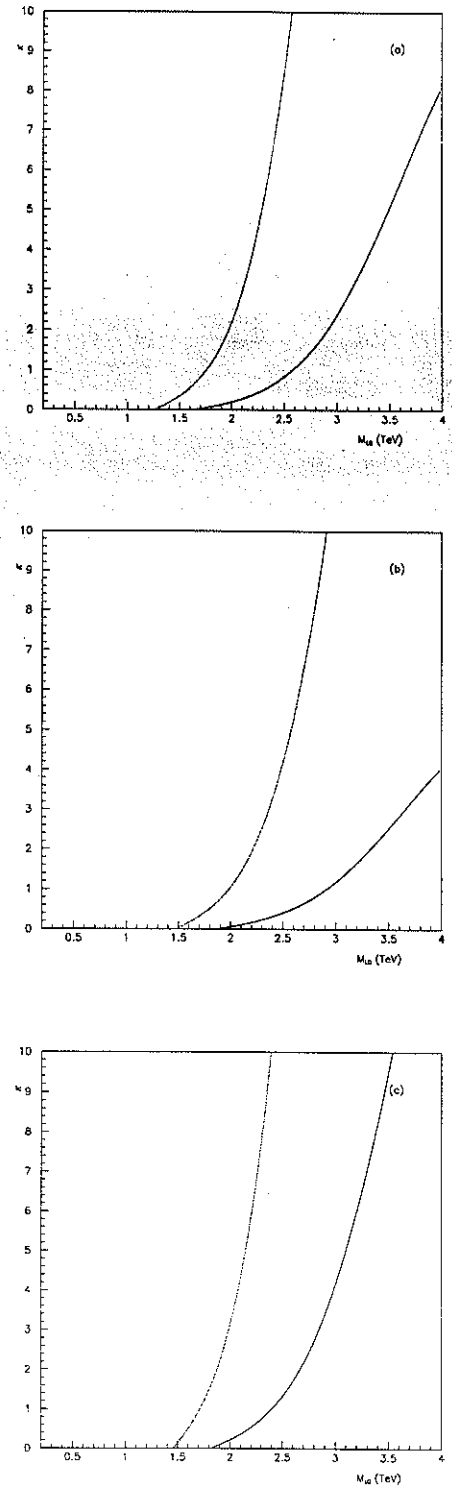

FIG. 15. 95% excluded regions in the plane κ–M_{lq} from the single leptoquark analysis for an integrated luminosity of 10/100 fb^{-1} (solid/dotted line) and the leptoquarks: (a) S_{1L} and S_3^0; (b) S_{1R}, R_{2L}^1, and R_{2R}^1; (c)S_3^+, R_{2R}^2, $\tilde{R}_2^1$, and $\tilde{S}_{1R}$.